

## Simple model for deriving *sdg* interacting boson model Hamiltonians: <sup>150</sup>Nd example

Y. D. Devi and V. K. B. Kota

Physical Research Laboratory, Ahmedabad 380 009, India

(Received 15 June 1992)

A simple and yet useful model for deriving *sdg* interacting boson model (IBM) Hamiltonians is to assume that single-boson energies derive from identical particle (*pp* and *nn*) interactions and proton, neutron single-particle energies, and that the two-body matrix elements for bosons derive from *pn* interaction, with an IBM-2 to IBM-1 projection of the resulting *p-n sdg* IBM Hamiltonian. The applicability of this model in generating *sdg* IBM Hamiltonians is demonstrated, using a single-*j*-shell Otsuka-Arima-Iachello mapping of the quadrupole and hexadecupole operators in proton and neutron spaces separately and constructing a quadrupole-quadrupole plus hexadecupole-hexadecupole Hamiltonian in the analysis of the spectra, *B*(*E2*)'s, and *E4* strength distribution in the example of <sup>150</sup>Nd.

PACS number(s): 21.60.Fw, 21.10.-k, 23.20.-g, 27.70.+q

In order to make progress in applying the *sdg* interacting boson model (IBM), which is demonstrated to be useful [1–10] in analyzing hexadecupole (*E4*) properties of nuclei, it is essential that one derives *sdg* Hamiltonians with some microscopic input, so that the number of free parameters [3 single-particle energies (SPE's) and 32 two-body matrix elements (TBME's)] will reduce to a minimal number (say 4–6). Broadly speaking, two approaches to this rather complicated problem are available: (i) phenomenological, and (ii) microscopic (based on the shell model and its relatives). The symmetry defined Hamiltonian  $H_{\text{sym}}$  of Devi *et al.* [3,4,9,11], the boson surface delta interaction  $H_{\text{BSDI}}$  of Chen *et al.* [12], and the Hamiltonian  $H_{\text{com}}$  based on the commutator method given by Kuyucak *et al.* [5,8] belong to the first class, while the Otsuka-Arima-Iachello (OAI) [13] mapped and IBM-2 to IBM-1 projected Hamiltonian  $H_{\text{OAI-proj}}$  proposed by Devi [3], the seniority transformed Dyson boson mapped and IBM-2 to IBM-1 projected Hamiltonian  $H_{\text{DYS-proj}}$  of Navratil and Dobes [14], and the single-*j*-shell seniority mapped Hamiltonian  $H_{\text{OAI-full}}$  of Yoshinaga [15] belong to the second class. Yoshinaga's  $H_{\text{OAI-full}}$  Hamiltonian is not useful in analyzing real nuclei unless it is extended to multi-*j*-shell cases, and also to proton-neutron systems. These extensions render the mapping procedure rather complicated, as there is no unique correspondence between four-fermion and two-boson states. This problem can be circumvented by adopting the model where one assumes that *single-boson energies derive from identical particle (pp and nn) interactions and proton and neutron single-particle energies, and the two-body matrix elements for bosons derive from pn interaction and carrying out an IBM-2 to IBM-1 projection of the re-*

*sulting p-n sdg IBM Hamiltonian.* This model [hereafter referred to as SPE(*pp + nn*)-TBME(*pn*)-proj] was recently used by Navratil and Dobes [14], together with the similarity transformed Dyson boson mapping in the multi-*j*-shell case, to give a reasonably good description of the spectroscopic properties (spectra, *E2*, and *E4*) of vibrational <sup>148</sup>Sm, nearly rotational <sup>150</sup>Nd, and  $\gamma$ -unstable <sup>196</sup>Pt nuclei. However, it is not clear whether the agreements obtained by Navratil and Dobes are due to the elaborate multi-*j*-shell mapping scheme they used or the model SPE(*pp + nn*)-TBME(*pn*)-proj employed. In order to conclusively establish the latter, in this report, using a simple single-*j*-shell OAI mapping in the above model, an IBM-1 Hamiltonian is derived, and the spectra, *B*(*E2*) values, and *E4* strength distribution are analyzed in the example of <sup>150</sup>Nd.

In order to construct *sdg* Hamiltonians with a microscopic (shell model) basis, one has to start with proton-neutron (*p-n*) degrees of freedom. Then, using the simple model SPE(*pp + nn*)-TBME(*pn*)-proj [3,14] and employing a quadrupole-quadrupole plus hexadecupole-hexadecupole form for the *p-n* force, the *p-n sdg* IBM Hamiltonian takes the form

$$H_{pn\ sdg\ IBM} = \sum_{\rho=\pi,\nu} (\epsilon_{d\rho} \hat{n}_{d\rho} + \epsilon_{g\rho} \hat{n}_{g\rho}) + \kappa_{\pi\nu}^{(2)} Q_{\pi}^2 \cdot Q_{\nu}^2 + \kappa_{\pi\nu}^{(4)} Q_{\pi}^4 \cdot Q_{\nu}^4. \quad (1)$$

In (1),  $\hat{n}_{d\rho}$  and  $\hat{n}_{g\rho}$  are *d* and *g* boson number operators for  $\rho=\pi$  for proton bosons and  $\nu$  for neutron bosons. Similarly,  $\epsilon_{d\rho}$ ,  $\epsilon_{g\rho}$ ,  $\kappa_{\pi\nu}^{(2)}$ , and  $\kappa_{\pi\nu}^{(4)}$  are free parameters. Using the OAI correspondence [13],

$$\begin{aligned} |(j_{\rho})^{2N_{\rho}}, v_{\rho}=0, J_{\rho}=0\rangle &\leftrightarrow |n_{s;\rho}=N_{\rho}, L_{\rho}=0\rangle, \\ |(j_{\rho})^{2N_{\rho}}, v_{\rho}=2, J_{\rho}=2\rangle &\leftrightarrow |n_{s;\rho}=N_{\rho}-1, n_{d;\rho}=1, L_{\rho}=2\rangle, \\ |(j_{\rho})^{2N_{\rho}}, v_{\rho}=2, J_{\rho}=4\rangle &\leftrightarrow |n_{s;\rho}=N_{\rho}-1, n_{g;\rho}=1, L_{\rho}=4\rangle, \end{aligned}$$

where  $2\Omega_{\pi}$  ( $2\Omega_{\nu}$ ) and  $N_{\pi}$  ( $N_{\nu}$ ) are the shell degeneracy and boson numbers for protons (neutrons) respectively

$[j_\rho = (2\Omega_\rho - 1)/2]$ , and equating the matrix elements of multipole operators in fermion  $[r_\rho^\lambda Y_\mu^\lambda(\theta_\rho, \phi_\rho)]$  and boson  $(Q_{\mu;\rho}^\lambda)$  spaces, one obtains the effective charges  $e_{ll';\rho}^{(\lambda)}$  that define  $Q_{\mu;\rho}^\lambda$ . They are [10]

$$e_{l0;\rho}^{(\lambda)} = e_{0l;\rho}^{(\lambda)} = \left[ \frac{2(\Omega_\rho - N_\rho)}{\Omega_\rho(\Omega_\rho - 1)(2\lambda + 1)} \right]^{1/2},$$

$$e_{ll';\rho}^{(\lambda)} = e_{l'l;\rho}^{(\lambda)} = \mp \left[ \frac{\Omega_\rho - 2N_\rho}{\Omega_\rho - 2} \right] \left[ \frac{4(2l + 1)(2l' + 1)}{(2\lambda + 1)} \right]^{1/2} \begin{Bmatrix} l & l' & \lambda \\ j_\rho & j_\rho & j_\rho \end{Bmatrix}, \quad l \neq l' \quad \text{and } \lambda = 2, 4. \quad (2)$$

The minus sign for  $e_{ll';\rho}^{(\lambda)}$  in (2) is for particle bosons [fermion number  $N_f \leq \Omega_\rho$ ,  $N_\rho = N_f/2$ ] and the plus sign is for hole bosons [fermion number  $N_f \geq \Omega_\rho$ ,  $N_\rho = (2\Omega_\rho - N_f)/2$ ]. The factors  $\langle j_\rho || r_\rho^\lambda Y_\mu^\lambda(\theta_\rho, \phi_\rho) || j_\rho \rangle$  that appear in the mapping are not shown in (2), and they are absorbed in the free parameters  $\kappa_{\pi\nu}^{(\lambda)}$  in (1). Note that  $(j_\pi, j_\nu)$  take the values  $(31/2, 43/2)$  and  $(43/2, 57/2)$  for rare earths and actinides respectively. Now, carrying out an IBM-2 to IBM-1 projection [16] by assuming that the low-lying levels belong to the  $F$  spin [17]  $F = F_{\max} = (N_\pi + N_\nu)/2$ , and using the simple result that

$$\langle FF_Z | e_\pi (b_\pi^\dagger \tilde{b}_\pi) + e_\nu (b_\nu^\dagger \tilde{b}_\nu) | FF_Z \rangle = [(e_\pi N_\pi + e_\nu N_\nu)/N] \langle FF | b^\dagger \tilde{b} | FF \rangle,$$

$F_Z = (N_\pi - N_\nu)/2$  (IBM-1 states correspond to  $F = F_Z = N/2$ ,  $N = N_\pi + N_\nu$ ), which follows from the Wigner-Eckart theorem in  $F$ -spin space, the OAI mapped and IBM-2 to IBM-1 projected Hamiltonian  $H_{\text{OAI-proj}}$  is

$$H_{\text{OAI-proj}} = \varepsilon_d \hat{n}_d + \varepsilon_g \hat{n}_g + \kappa_2 (Q_\pi^2 \cdot Q_\nu^2)_{\text{proj}} + \kappa_4 (Q_\pi^4 \cdot Q_\nu^4)_{\text{proj}},$$

$$\varepsilon_d = \sum_\rho \varepsilon_{d\rho} N_\rho / N, \quad \varepsilon_g = \sum_\rho \varepsilon_{g\rho} N_\rho / N, \quad \kappa_r = \frac{N_\pi N_\nu}{N(N-1)} \kappa_{\pi\nu}^{(r)}, \quad r = 2, 4, \quad (3)$$

$$(Q_\pi^\lambda Q_\nu^\lambda)_{\text{proj}} =: \left[ \sum_{l_1 l_2} e_{l_1 l_2; \pi}^{(\lambda)} (b_{l_1}^\dagger \tilde{b}_{l_2})^{(\lambda)} \right] \cdot \left[ \sum_{l_3 l_4} e_{l_3 l_4; \nu}^{(\lambda)} (b_{l_3}^\dagger \tilde{b}_{l_4})^{(\lambda)} \right]; \quad \lambda = 2, 4.$$

In (3),  $::$  denotes normal ordering. Assuming  $\varepsilon_d$  and  $\varepsilon_g$  to be free parameters (instead of deriving them from  $pp$  and  $nn$  interactions) the Hamiltonian  $H_{\text{OAI-proj}}$  is used to study the spectroscopy of  $^{150}\text{Nd}$ ; the boson number  $N = 9$  with  $N_\pi = 5$  and  $N_\nu = 4$ . Furthermore, based on the success of earlier calculations for Sm isotopes [9] and nuclei in the Os-Pt region [3,4], the spherical basis defined by  $n_s$ ,  $n_d$ , and  $n_g$  with the restrictions  $n_s \geq n_s^{\min}$  and  $n_g \leq n_g^{\max}$ , where  $n_s^{\min} = 2$  and  $n_g^{\max} = 2, 3$ , are adopted. Although calculations with both  $n_g^{\max} = 2$  and 3 are performed (for Sm and Pt-Os isotopes, the  $n_g^{\max} = 2$  restriction is used [3,4,9]) for comparison with the results given in [14], where  $H_{\text{DYS-proj}}$  is used with  $n_g^{\max} = 3$ , only the  $n_g^{\max} = 3$  results are discussed. It should be mentioned that the  $n_g^{\max} = 2$  results are essentially the same as the  $n_g^{\max} = 3$  results, the latter being slightly better. With  $n_s^{\min} = 2$  and  $n_g^{\max} = 3$  restrictions, the matrix dimensions for  $L = 0, 1, 2, 3, 4, 5$ , and 6 are 65, 90, 203, 208, 286, 260, and 294, respectively.

In order to calculate  $E2$  and  $E4$  properties the consistent  $Q^2, Q^4$  formalism is adopted, which leads to the following multipole operators ( $T^{E\lambda}$ ):

$$T_\mu^{E\lambda} = \left[ \sum_{\rho=\pi,\nu} e_\rho^{(\lambda)} Q_{\rho;\mu}^\lambda \right]_{\text{proj}} = \sum_{l,l'=0,2,4} \left[ \frac{1}{N} \sum_{\rho=\pi,\nu} N_\rho e_\rho^{(\lambda)} e_{ll';\rho}^{(\lambda)} \right] (b_l^\dagger \tilde{b}_{l'})_\mu^\lambda, \quad \lambda = 2, 4. \quad (4)$$

TABLE I.  $B(E2)$  values for  $^{150}\text{Nd}$ .

$L_i \rightarrow L_f$	Expt. <sup>a</sup>	$B(E2; L_i \rightarrow L_f) (10^4 e^2 \text{fm}^4)$	
		OAI-proj <sup>b</sup>	DYS-proj <sup>c</sup>
$2_1^+ \rightarrow 0_1^+$	$0.563 \pm 0.002$	0.537	0.560
$4_1^+ \rightarrow 2_1^+$	$0.819 \pm 0.038$	0.879	0.810
$6_1^+ \rightarrow 4_1^+$	$0.980 \pm 0.09$	0.934	0.883
$0_2^+ \rightarrow 2_1^+$	$0.208 \pm 0.009$	0.227	0.071
$2_\beta^+ \rightarrow 4_1^+$	$0.095 \pm 0.028$	0.037	0.033
$2_\beta^+ \rightarrow 2_1^+$	$0.036 \pm 0.017$	0.069	0.004
$2_\beta^+ \rightarrow 0_1^+$	$0.0024 \pm 0.0005$	0.001	0.012
$2_\gamma^+ \rightarrow 2_1^+$	$0.034 \pm 0.007$	0.001	0.073
$2_\gamma^+ \rightarrow 0_1^+$	$0.015 \pm 0.0009$	0.011	0.012

<sup>a</sup>Reference [18].

<sup>b</sup>Present calculation.

<sup>c</sup>Reference [14].

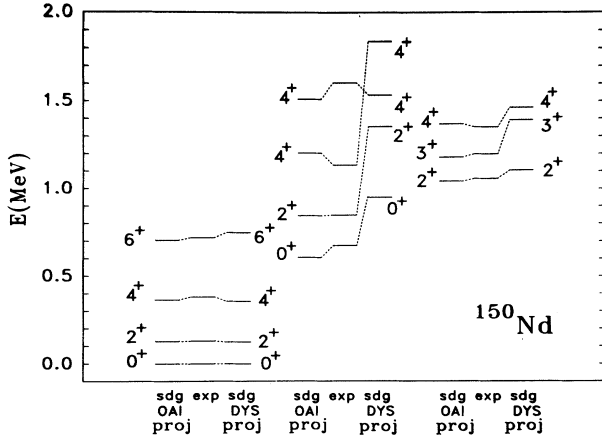


FIG. 1. Experimental and calculated energy levels for  $^{150}\text{Nd}$ . Experimental data are from [18]. The results calculated using  $H_{\text{OAI-proj}}$  (present calculations) and  $H_{\text{DYS-proj}}$  [14] in *sdg* space with  $n_g^{\text{max}}=3$  are labeled as *sdg*-OAI-proj and *sdg*-DYS-proj, respectively. It is important to note that the simple  $H_{\text{OAI-proj}}$  gives results that are in closer agreement to data, compared to those obtained with a more microscopic  $H_{\text{DYS-proj}}$ , although the number of free parameters are the same in both calculations.

The effective charges  $e_{ll';p}^{(\lambda)}$  are the same as the ones used in the Hamiltonian (3), and they are defined in (2). The  $e_{\pi}^{(\lambda)}$ ,  $e_{\nu}^{(\lambda)}$  are the two free parameters in  $T^{E\lambda}$ .

The calculated spectrum for  $^{150}\text{Nd}$  is shown in Fig. 1, and it is compared with data, as well as with the calculations of Navratil and Dobes [14]. The rms deviation from experimental energy levels is 37 keV. The description of the data obtained with  $H_{\text{OAI-proj}}$  is as good as, if not somewhat better than, the  $H_{\text{DYS-proj}}$ . The parameters in the calculations are (in MeV)  $\varepsilon_d=0.556$ ,  $\varepsilon_g=1.378$ ,  $\kappa_2=-0.498$ , and  $\kappa_4=-0.859$ ; the  $\varepsilon_d$  and  $\varepsilon_g$  values are from Ref. [14]. The  $B(E2)$  values are calculated using the  $E2$  operator (4) with  $e_{\pi}^{(2)}=1.95 \times 10^2 e \text{ fm}^2$  and  $e_{\nu}^{(2)}=-5.04 \times 10^2 e \text{ fm}^2$ , and the results are given in Table I. Once again, the agreements between data and the present calculations are as good as those [14] in which a more elaborate mapping procedure is used. The nucleus  $^{150}\text{Nd}$  is one of the few nuclei in the  $100 \leq A \leq 200$  region where  $E4$  strength distribution [ $B(E4; 0_{g.s.}^+ \rightarrow 4_i^+)$ ] for  $4^+$  levels up to  $\sim 3$  MeV] is measured [1], the other two being  $^{112}\text{Cd}$  [2] and  $^{156}\text{Gd}$  [19]. Therefore, as a further test of the model  $\text{SPE}(pp+nn)$ -TBME(*pn*)-Proj, which is used in deriving  $H_{\text{OAI-proj}}$ , the  $E4$  strength distribution in  $^{150}\text{Nd}$  is constructed using the  $E4$  operator (4) with  $e_{\pi}^{(4)}=7.486 \times 10^4 e \text{ fm}^4$  and  $e_{\nu}^{(4)}=-9.94 \times 10^4 e \text{ fm}^4$ , and the results are compared with the data in Fig. 2. Shown also are the results obtained with  $H_{\text{DYS-proj}}$  [14] and Hartree-Bose plus Tamn-Dancoff approximation (HB+TDA) calculations of Wu et al. [1]. The details of the HB+TDA calculations where a phenomenological Hamiltonian is employed are given in [1]. From Fig. 2 it is seen that (i) the  $H_{\text{OAI-proj}}$  calculation, although it reproduces the largest  $0_{g.s.}^+ \rightarrow 4_1^+$  strength, underestimates the strength between 2 and 3

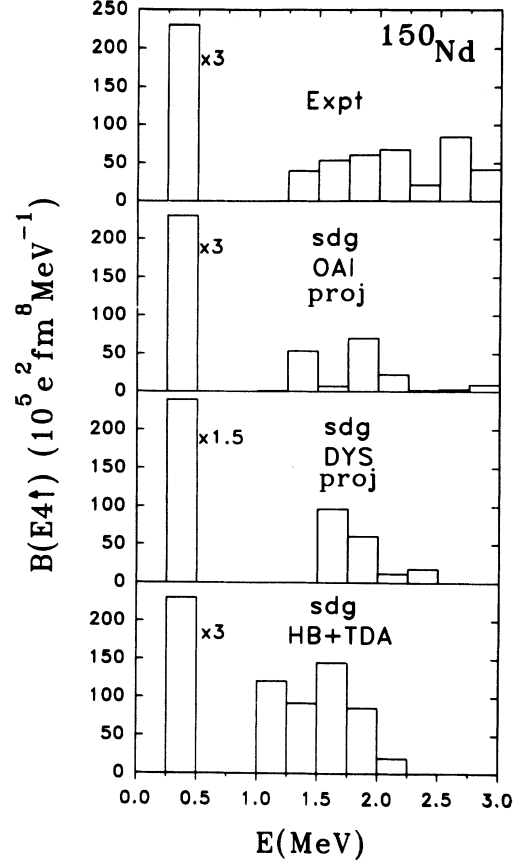


FIG. 2.  $E4$  strength distributions in  $^{150}\text{Nd}$  as measured in experiment [1] and the results of *sdg* IBM calculations. (i) Matrix diagonalization calculations with  $H_{\text{OAI-proj}}$  denoted as *sdg*-OAI-proj (present calculation); (ii) matrix diagonalization calculations with  $H_{\text{DYS-proj}}$  denoted as *sdg*-DYS-proj [14]; (iii) HB+TDA calculations denoted as *sdg*-HB+TDA [1]. Shown in the figure is  $B(E4\uparrow)$  strength/MeV with 0.25 MeV bin size;  $B(E4\uparrow)=B(E4; 0_{g.s.}^+ \rightarrow 4_i^+)$ . Note that the strength in the bin (0.25–0.5) MeV must be multiplied by the factors 3, 3, 1.5, and 3 in experiment, *sdg*-OAI-proj, *sdg*-DYS-proj, and *sdg*-HB+TDA calculations respectively.

MeV, (ii) the  $H_{\text{DYS-proj}}$  underestimates the overall strength by a factor of 2, and also the observed fragmentation between 2 and 3 MeV is not properly described, and (iii) the HB+TDA calculation describes the fragmentation of the  $E4$  strength reasonably well, in spite of the fact that it overestimates the strength between 1 and 2 MeV and predicts none between 2.25 and 3 MeV, although experimentally there is sizeable strength in this domain. From this comparison it is clear that the observed  $E4$  strength distribution in  $^{150}\text{Nd}$  is reasonably well described by the *sdg* IBM, although the calculation HB+TDA overestimates and  $H_{\text{OAI-proj}}$  underestimates the strength between 2 and 3 MeV. However, considering the microscopic nature of the model  $\text{SPE}(pp+nn)$ -TBME(*pn*)-Proj employed in constructing  $H_{\text{OAI-proj}}$  and the  $E4$  transition operator, together with the agreements shown in Fig. 2, it can be concluded that it is a viable model for studying  $E4$  properties.

The results given for spectra,  $B(E2)$  values, and  $E4$  strength distributions for  $^{150}\text{Nd}$  clearly indicate that the simple model  $\text{SPE}(pp + nn)\text{-TBME}(pn)\text{-proj}$  should be an essential ingredient of any microscopic procedure for

deriving  $sdg$  IBM Hamiltonians. In order to conclusively establish this result, it is desirable to have a more systematic set of calculations employing the above model for a variety of nuclei.

- 
- [1] H. C. Wu, A. E. L. Dieperink, O. Scholten, M. N. Harakeh, R. De Leo, M. Pignanelli, and I. Morrison, *Phys. Rev. C* **38**, 1638 (1988).
- [2] R. De Leo, N. Blasi, S. Micheletti, M. Pignanelli, W. T. A. Borghols, J. M. Schippers, S. Y. Vander Werf, G. Maino, and M. N. Harakeh, *Nucl. Phys.* **A504**, 109 (1989).
- [3] Y. D. Devi, Ph.D. thesis, Gujarat University, 1991.
- [4] Y. D. Devi and V. K. B. Kota, in *Proceedings of the DAE Symposium on Nuclear Physics*, Bombay, 1991, edited by S. Kailas and P. Singh (Library & Information Services Division, BARC, Bombay, 1991), Vol. 34B, p. 47.
- [5] S. Kuyucak, V. S. Lac, I. Morrison, and B. R. Barrett, *Phys. Lett. B* **263**, 347 (1991).
- [6] J. Wesseling, C. W. De Jager, J. B. Vanderlaan, H. Devries, and M. N. Harakeh, *Nucl. Phys.* **A535**, 285 (1991).
- [7] A. Sethi, N. M. Hintz, D. N. Mihailidis, A. M. Mack, M. Gazzaly, K. W. Jones, G. Pauletta, L. Santi, and D. Goutte, *Phys. Rev. C* **44**, 700 (1991).
- [8] S. Kuyucak, I. Morrison, and T. Sebe, *Phys. Rev. C* **43**, 1187 (1991).
- [9] Y. D. Devi and V. K. B. Kota, *Phys. Rev. C* **45**, 2238 (1992).
- [10] Y. D. Devi and V. K. B. Kota, *Phys. Rev. C* **46**, 370 (1992).
- [11] Y. D. Devi, V. K. B. Kota, and J. A. Sheikh, *Phys. Rev. C* **39**, 2057 (1989).
- [12] H. T. Chen, L. L. Kiang, C. C. Yang, L. M. Chen, T. L. Chen, and C. W. Jiang, *J. Phys. G* **12**, L217 (1986); H. T. Chen, R. W. Richardson, L. L. Kiang, Y. Tzeng, P. K. Teng, G. C. Kiang, C. W. Wong, S. F. Tsai, E. K. Lin, and A. Arima, *ibid.* **14**, L205 (1988).
- [13] T. Otsuka, A. Arima, and F. Iachello, *Nucl. Phys.* **A309**, 1 (1978).
- [14] P. Navratil and J. Dobes, *Nucl. Phys.* **A532**, 223 (1991).
- [15] N. Yoshinaga, *Nucl. Phys.* **A493**, 323 (1989); N. Yoshinaga, *Nucl. Phys.* **A503**, 65 (1989).
- [16] W. Frank and P. O. Lipas, *J. Phys. G* **16**, 1653 (1990).
- [17] P. O. Lipas, P. von Brentano, and A. Gelberg, *Rep. Prog. Phys.* **53**, 1355 (1990).
- [18] E. der Mateosian, *Nucl. Data Sheets*, **48**, 345 (1986).
- [19] P. B. Goldhoorn, M. N. Harakeh, Y. Iwasaki, L. W. Put, F. Zwarts, and P. Van Isacker, *Phys. Lett.* **103B**, 291 (1981).